Hydrogen Adsorption in Thin Films of Prussian Blue Analogues

Dali Yang[1]*, Vivian Ding[1], Junhua Luo[2], Robert Currier[3], Steve Obrey[3], Yusheng Zhao[2]

[1]Materials Science Division, [2]Los Alamos Neutron Scattering Center, [3]Chemistry Division, Los Alamos National Laboratory, Los Alamos, New Mexico, USA 87544
*(*Corresponding author. Email address: dyang@lanl.gov, Tel: 505-665-4054, Fax: 505-667-8109)*

Abstract

Quartz crystal microbalance with dissipation (QCM-D) measurement was used to investigate the kinetics of molecular hydrogen adsorption into thin films of the Prussian blue analogue $Cu_3[Co(CN)_6]_2$ at ambient conditions. Although the equilibrium adsorption seems to be independent of the thickness, the adsorption rate substantially decreases with the thickness of the films. In addition, the reversibility of H_2 adsorption into the $Cu_3[Co(CN)_6]_2$ films was investigated. The results indicate that the $Cu_3[Co(CN)_6]_2$ mainly interacts with H_2 molecules physically. The highest measured H_2 uptake by $Cu_3[Co(CN)_6]_2$ films was obtained when the gas phase was stagnant inside the testing cell. However, the unusual high H_2 uptake measured by QCM-D calls into question the reliability of the method.

LAUR number - 08-06013

1. Introduction

Prussian blue analogues consist of structures based on a simple cubic $M[M'(CN)_6]$ framework, in which $[M'(CN)_6]^{n-}$ complexes are connected *via* octahedrally coordinated, nitrogen-bond M^{n+} ions. Upon dehydration (heating), the metal ligand framework produces several perspective binding sites for H_2, including open coordination sites in the M^{2+} ions. The robust nature of the framework, facilitated by the short and rigid connectivity and three-dimensionality, enables the open porous structure to be retained leaving coordinatively unsaturated metal centres.[1-3] Kaye and Long suggested that the availability of eight Cu^{2+} binding sites per unit cell in $Cu_3[Co(CN)_6]_2$ would be advantageous for H_2 sorption.[3] The binding energy of these analogues is around 5 – 10 KJ/mol.[1-3]

To fully utilize the high surface area of the metal organic frameworks (MOFs), it may ultimately prove necessary to fabricate MOFs into the geometries with the high interfacial area (e.g., thin film) and/or complex structures (e.g., composite membranes and hollow fibers). It is well known that the interfacial properties of materials can differ significantly from the bulk properties.[4-8] Therefore, understanding how the interfacial behavior of thin film MOFs differs from their bulk form is important.

In contrast to volumetric measurements, which are mainly carried out on bulk materials (typically requiring > 10 mg and a long times > 100 hrs to perform measurements),[1-3,9-13] solid-state sensors can provide significant advantages for detecting mass uptake. These devices can be easily interfaced with the process stream and can be readily replaced. For example, a quartz crystal microbalance (QCM) show very high sensitivity (up to $<10^{-9}$ g/cm^2) to mass changes on the surface of the oscillating quartz crystal. In the past 30 years, many researchers have used QCM as an accurate, sensitive, and fast analytical tool for studying absorption/desorption, gas

sensing, and pollutant detection in many materials (e.g., metals, nanoporous silica, carbon nanotubes, zeolites, alloys, polymers, and etc.).[14-32]

In this study, the objective was to take the advantage of the QCM sensitivity to study the kinetics of H_2 soprtion in MOF thin films. As a consequence of the low water content and dehydration temperature of the Prussian blue analogues, $Cu_3[Co(CN)_6]_2$, was chosen as a model compound.[2] By changing film thickness, film mass, and test conditions, the effects of morphology and operating condition could be investigated. However, ultra high H_2 uptake was detected under ambient conditions, which makes us question the reliability of the measurement as currently understood. Clearly, more in-depth study and fundamental understanding are needed before we can confidently use this technique for the kinetics of gas adsorption.

2. Background on the QCM-D Technique

The QCM-D technique is based on a disc-shaped, AT-cut piezoelectric quartz crystal with Au electrodes deposited on both faces. For a Q-sense quartz plate, the Au electrode on the one side of quartz is smaller than the other side. The active surface area (~0.2 cm^2) is determined by the small area of the electrode. The crystal is excited to oscillation in the thickness shear mode at its fundamental and overtone resonant frequencies (*f*) by applying a voltage across the electrodes near the resonant frequency. A small mass added to the electrodes *(Δm)* induces a decrease in the resonant frequency *(Δf)*, which is proportional to Δ*m* based on Sauerbrey equation[33]

$$\Delta m = -\frac{A\sqrt{\rho_Q G_Q}\Delta f}{2 f_o^2} \qquad (1)$$

where A is the active surface area, ρ_Q and G_Q are the density and the shear modules of the quartz plate, and f_o is the resonance frequency of unloaded quartz plate. Using Eq. 1, the adsorbed mass *(Δm)* can be deduced from a linear relation fit to the shift in the resonant frequency *(Δf):*

$$\Delta m_{QCM} = -C_{QCM}\Delta f / n \qquad (2)$$

where C_{QCM} (=17.67 ng cm^{-2} Hz^{-1} at f = 5MHz) is the mass sensitivity constant and *n* (=1,3,..) is the overtone number. However, both Eq. 1 and Eq. 2 are valid when the following conditions are met *a)* added mass is small compared to the weight of the crystal quartz (< 2 mass%), and *b)* the film is rigid without slip on the electrode and evenly distributed over the active area of the quartz.

The dissipation factor (*D*) is the inverse of the better known Q factor, defined by:

$$D = \frac{1}{Q} = \frac{E_{Dissipated}}{2\pi E_{Stored}} \qquad (3)$$

$$where\ Q = \pi f \tau$$

where $E_{Dissipated}$ and E_{Stored} are the energy dissipated and stored during one period of oscillation, respectively. When the driving power (at frequency *f*) to the excited quartz plate is switched off at time = 0, the amplitude of oscillation decays as an exponentially damped sinusoid at the decay time constant of τ (sec^{-1}). Consequently, *D* is the sum of all mechanisms that dissipate energy from the oscillating system such as friction and viscous losses. In general, viscous materials dissipate more energy than rigid ones.

3. Experimental

3.1 Syntheses

A solution of $Cu(NO_3)_2 \cdot 2.5H_2O$ (4.1866 g, 18 mmol) in 100 mL H_2O was slowly added into a solution of $K_3[Co(CN)_6]$ (3.3234 g, 10 mmol) in 100 mL H_2O with magnetically stirring. The mixture was then placed in an furnace at 90 °C for 10 hours. The resulting blue precipitate was filtered and washed thoroughly with H_2O (10 mL) 3 times. The yield was 95% (3.7185 g) based based on Co mass. Both $Cu(NO_3)_2 \cdot 2.5H_2O$ and $K_3[Co(CN)_6]$ (95%) were acquired from Aldrich and used as received. The synthesized $Cu_3[Co(CN)_6]_2$ powder was washed using methanol a few times, and then vacuum dried at 120 °C for more than 8 hours. The dried powder was sealed in a glass bottle.

3.2 Characterization

To verify the phase purity of the as-synthesized compound, elemental analyses of C, H and N were performed on a Perkin-Elmer 240C elemental analyzer, powder X-ray diffraction (PXRD) patterns were collected on a Rigaku, Ultima III instrument (Bragg-Brentano geometry), and mid-infrared (400-4000 cm^{-1}) spectra were collected using a Mattson Genesis II FTIR spectrometer operating at a resolution of 2 cm^{-1}. The thermal stability of the $Cu_3[Co(CN)_6]_2$ powder was determined using a thermo-gravimetric analyzer (NETZSCH STA 449C and TASC 414/4 controller), under a dry nitrogen and air atmosphere (at 30 ml/min flowrate) over a temperature range of 25 – 600 °C and at a heating rate of < 1 K/min. Prior to the N_2 testing, the sample chamber was evacuated for a few minutes at room temperature (~23 °C). The weight loss/temperature curve was measured. Simultaneously, the signal of a differential scanning calorimeter was recorded.

3.3 Thin film preparation and characterization

To prepare the $Cu_3[Co(CN)_6]_2$ thin film, 0.5 gram of $Cu_3[Co(CN)_6]_2$ fine powder was dispersed into 10 - 15 ml methanol to form a suspension. After the large particles settled down for a few minutes, the top portion of the suspension, containing fine particles, was used to prepare the films. Drops of the suspension were cast on the pre-determined weighed and cleaned electrode using a micro-pipette (< 10 μl). The thin film was formed as the solvent was evaporated under vacuum at ~100 °C. The weight of deposited $Cu_3[Co(CN)_6]_2$ was measured by the difference of the electrode weight before and after the deposition. Films typically weighed from 10 to 32 microgram (< 0.02 mass% of the electrode weight. The crystal structure of the coated films was verified using X-ray diffraction. The thickness of the $Cu_3[Co(CN)_6]_2$ films was determined using Nikon mm-60 measuring microscope (Nikon, Japan). The thickness of the films was typically less than 5 μm. The thinnest film was ~0.7± 0.3 μm. The analytical error on the thickness was ~25 %.

3.4 Gas sorption apparatus

The gas sorption/desorption experiments were conducted using the QCM-D instrument (Q-sense, Inc.). The measurement chamber (D300) and electronic unit (QE 301) were purchased from Q-sense. AT-cut quartz crystal coated with 100 nm Au layer was the sensor electrode (QSX 301, Q-sense, Inc.). The software QSoft (Q-sense) was used to acquire changes in the frequency, dissipation factor, and temperature. Ultra high pure H_2 (99.9995%) was purchased from

Matheson Tri-Gas. A mass flow controller Stay – III (Sierra Instruments, Inc) was used to control the gas flow rate when tests were conducted at a constant flow rate (0 - >30 ml/min at the ambient conditions). The operational pressure varied from vacuum to slightly above the ambient pressure (~590 ± 10 torr). The chamber temperature was controlled at 23.5 °C within ± 0.05 °C of accuracy. All of the ultra-pure gas was passed through two inline filters before feeding into the QCM chamber. One Baratron absolute pressure gauge (0 – 1000 torr) was mounted at the outlet of the QCM-D chamber to monitor the pressure change during the experiments.

3.5 Isothermal sorption experiment

Prior to casting the films, clean blank quartz crystals were tested at different experimental conditions for 4 overtones (5-35 MHz). In a typical test, the QCM chamber was pumped under dynamic vacuum (< 10^{-3} torr) for more than a few hours until the changes in the frequency *(*ΔF*)* and dissipation faction *(*ΔD*)* approached constants. Then, the QCM chamber was charged with the ultra-high pure H_2 above 600 torr within a few seconds. Once the chamber pressure was above 610 torr, we quickly equilibrated the pressure with the ambient pressure (~590 ± 15 torr) and then isolated the chamber from outside. However, when the chamber pressure changed from vacuum to the ambient pressure, a change in ΔF for the blank quartzes was observed. This value, slightly different for different quartz crystals, was typically in the range of 48 ± 5 Hz for F1 at 23.5 °C and was taken into count in the data analysis. The gas flow rate through the QCM chamber had neglect effect on both frequency *(*ΔF < 1 Hz) and dissipation factor *(*$\Delta D < 0.1 \times 10^{-6}$*)* for the uncoated quartz crystals when the flow rate changed from 0 to > 50 ml/min.

Once placed on the quartz crystals, the films were dried in a vacuum oven at ~100 °C for 16 – 24 hour, and then quickly loaded into the QCM-D chamber. Before the sorption test, the QCM chamber was further evacuated for a few hours until both frequency and dissipation factor reached a plateau. After the chamber was charged with H_2 up to the ambient pressure and then isolated from outside, the shifts on the frequencies and dissipation factors were recorded over the sorption process at the time intervals of 0.01 ~ 1.0 sec until both Δf and ΔD reached a steady-state. During this period, the pressure of the QCM chamber was also monitored. Following the sorption process, desorption was monitored by evacuating the QCM chamber until both shifts (Δf and ΔD) reached a plateau. All of the measurements were conducted at 23.5 ± 0.5 °C. By comparing the frequency of the coated films under the vacuum, we confirmed that the weight loss was typically less than < 5% of the original weight after the films were tested for more than 30 days.

We also conducted the isothermal sorption at different hydrogen flow rates. The experimental procedures were the identical as the above, except for the flow of H_2 through the QCM chamber (0 ~ >50 ml/min flow rate at ambient pressure).

4. Results and Discussion

4.1 Characterization of $Cu_3[Co(CN)_6]_2$ powder

In Figure 1 (a), we compare the powder X-ray diffraction (PXRD) patterns indexed from single crystal of $Cu_3[Co(CN)_6]_2.9H_2O$ and the as-synthesized $Cu_3[Co(CN)_6]_2.9H_2O$. The almost identical PXRD patterns confirmed the phase purity of the synthesized compound. Mid-infrared (400-4000 cm^{-1}) spectra in Figure 1(b) were collected for both hydrated and dehydrated samples.

The IR spectra clearly indicate that the water molecules were removed completely corresponding to the lack of a peak at ~ 3400 cm^{-1} after heating at 120 °C.

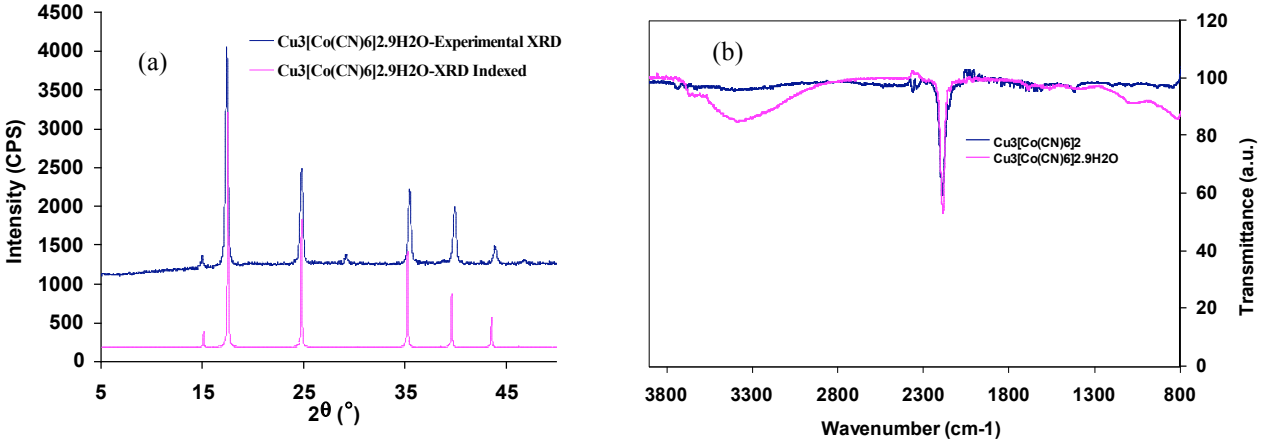

Figure 1. (a) PXRD patterns of single crystal (pink) and as-synthesized $Cu_3[Co(CN)_6]_2.9H_2O$ (blue) and (b) IR spectra of hydrate (purple) and dehydrated $Cu_3[Co(CN)_6]_2$ (blue).

The thermal stability of $Cu_3[Co(CN)_6]_2$ powder under N_2 and air were also investigated. The TGA and DSC results are shown in Figure 2(a) and 2(b), respectively, and suggest that the hydrated $Cu_3[Co(CN)_6]_2$ powder lost coordinated water below 120 °C and stable up to 260 °C. These results are consistent with prior studies.[2] The weight loss observed under N_2 appeared to be less than that under air when the heating temperature was less than 120 °C, which suggests a poorer stability of $Cu_3[Co(CN)_6]_2$ in the air environment than that in N_2 environment. After $Cu_3[Co(CN)_6]_2$ lost water in air, its weight continuously decreased during heating. Because of the oxidation occurring around 280 °C in air environment, the compound released an appreciable amount of heat whereas the compound seemed to adsorb some heat between 350 and 480 °C in N_2. The hydrothermal treatment ~120 ºC resulted in fine $Cu_3[Co(CN)_6]_2$ powder with nanometer size.

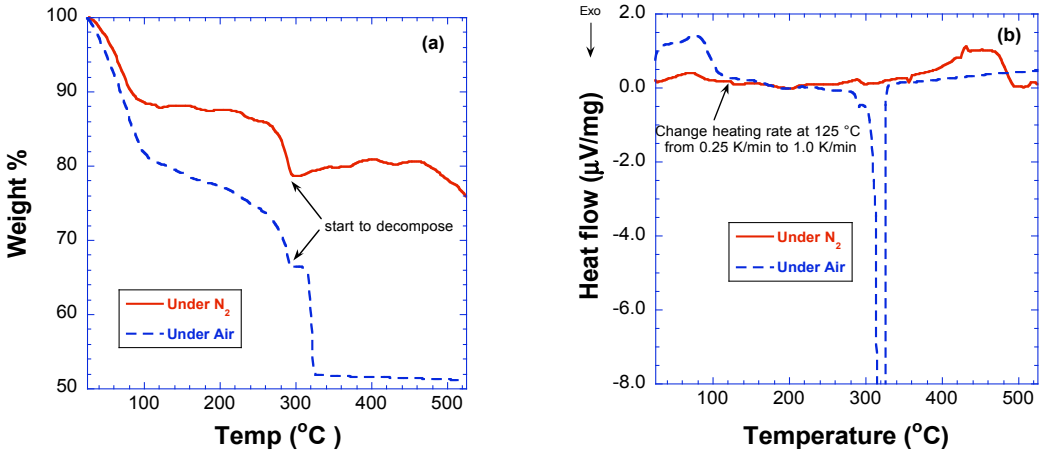

Figure 2. The thermal analysis results of $Cu_3[Co(CN)_6]_2$ powder under N_2 and air conditions (a) TGA results and (b) corresponding DSC results (the heating rate 0.25 K/min to 1 K/min).

4.2 Isothermal sorption

Figure 3(a) illustrates typical time evolution of the frequency shift when the films were exposed to H_2 at 23.5 °C. One qualitative feature of all measurements was that the amount of the adsorbed gases increased monotonically with time and reached a plateau, and showed distinct two processes as a function of time. However, the sorption kinetics appeared to vary from one sample to the others. To better illustrate the sample-to-sample variation, the normalized frequency shift ($\Delta F/\Delta F_{max}$) is plotted in Figure 3(b). The thinner films (<2.0 μm) reached 50% capacity less than one hour, whereas the thickest film (S6) took a few hours. Similar behavior was reported on the palladium (Pd) thin films interacting with H_2 by RaviPrakash et al.[34] who suggested that the film morphology strongly influenced the rate of sorption of the Pd thin film, but the plateau values were solely dependent on the mass of the materials. Furthermore, although the thickness of S4 is larger than that of samples S3, S5 and S8, the S4 sample gives the highest slope in its sorption curve at the early stage (< a few minutes). The result suggests that in addition to thickness, other factors such a grain size may also impact the kinetics of the sorption process in the thin films. We suspect that the largest mass of S4 may contribute to the fast kinetics.

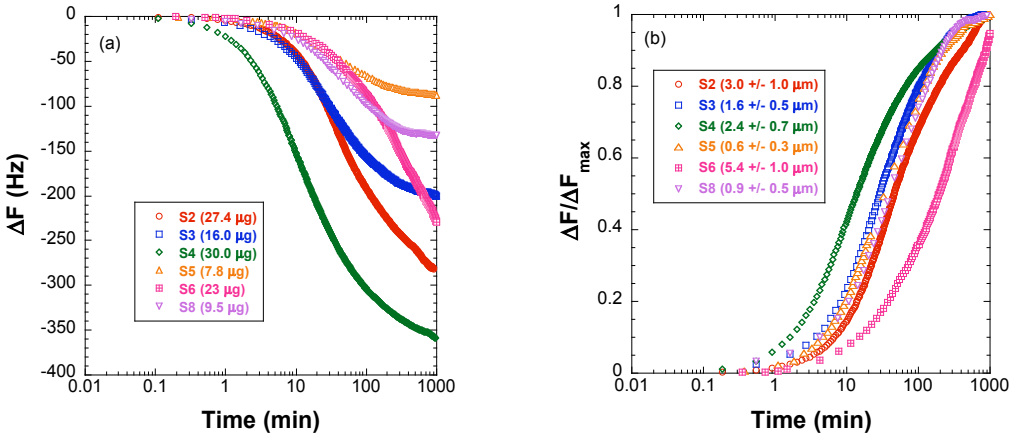

Figure 3. The illustrations of H_2 sorption behavior of several $Cu_3[Co_2(CN)_6]_2$ thin films at ambient conditions (23.5 ± 0.1 °C and < 520 torr) (a) and the plot of $\Delta F1/\Delta F1_{max}$ *vs.* time (b).

The sample weight, thickness, calculated added mass and H_2 mass uptake are summarized in Table I. The films (S3, S5, and S8) were relatively thin (< 2 μm) and uniform and three overtones (F1, F3/3 and F5/5) were detected and they overlapped fairly well. Therefore, the Sauerbrey equation can be used to calculate added masses of these samples (i.e. Δm). The H_2 uptake for the thin films is typically 0.5 – 1.0 wt% higher than that for the thicker films. This is similar to that found for Pd/H_2 sorption, the very high H_2 uptake was obtained for the thin Pd film coated on to the QCM electrode as well.[18] Frazier et al. suggested when the film thickness decreased the film became discontinuous and thus the surface/volume ratio was increases, which might increase the accessibility of the gas molecules, and resulted in a much higher H_2 uptake than that obtained in the thick films.[18] An alternative perspective is that inter-grain sorption is occurring and that the opportunity for grain boundary sorption is greater (per unit mass of film) in the thinner films.

However, the average H_2 mass uptake of the 6 samples reported here is about 4.4 ± 0.6

wt% at ambient conditions (23.5 °C and < 520 torr), which is much higher than what has been reported for the bulk material. Although the high sensitivity of the QCM and the thin film of the tested samples may allow us to detect the maximal H_2 capacity in $Cu_3[Co_2(CN)_6]_2$ thin films, a capacity which may exceed what can be achieved in bulk, a value of ~4.5 wt% H_2 at ambient conditions is suspect. The H_2 uptake by the same compound in bulk form reported in the literature is < 2.0 wt% at 77 K and <890 torr.[1,3,10] In order to thermodynamically stabilize H_2 at ambient conditions (~ 20 °C and 1 atm) ($\Delta H_{H2} = T\Delta S_{H2}$), the binding energy between H_2 and $Cu_3[Co_2(CN)_6]_2$ has to be as high as ~32 KJ/mol. However, the reported binding energy of these analogues is less than 10 KJ/mol at liquid nitrogen temperature. Therefore, the validity of the QCM-D measurement is questionable if the sorption is occurring at the usual sites within the framework. None-the-less, the experimental results reported above were shown to be reproducible. Hence, some additional contributions to sorption are suspected to be at play in order to produce such a large capacity change relative to the bulk measurement.

Table I. Summary of sample thickness, weight, added mass, and H_2 uptake by the $Cu_3[Co_2(CN)_6]_2$ thin films (23.5°C and < 520 torr).

Sample Label	Thickness (μm)	Sample weight[1] (μgram)	Sample weight[2] (μgram)	Δm_{Max} (μgram)	H_2 uptake (Wt%)
S2[3]	3.0	27.4	28 ± 1.0	1.03	3.86
S3	1.6	16.0	20 ± 1.0	0.77	4.84
S4	2.4	30.0	34 ± 1.0	1.39	4.65
S5	0.6	7.8	9 ± 1.0	0.32	4.66
S6[4]	5.4	23.0	26 ± 1.0	0.89	3.87
S8	0.9	9.5	10 ± 1.0	0.49	5.13

[1]: The sample weight inside the active area (~0.2 cm^2) on the quartz was calculated based on the frequency difference (under vacuum) before and after the film was coated to the surface of quartz. This weight was used in the H_2 uptake calculation.
[2]: This weight was measured directly using CAHN C-31 microbalance. The large weight was expected because it counted the entire sample coated on the quartz surface.
[3]: We only detected F1 and F3 for both S2 and S4. The calculation added mass using the Sauerbrey equation might result in some error.
[4]: Due to the large thickness and loose packing, we only detected the fundamental frequency (5 MHz) for S6. Its sorption took more than 1400 minutes to reach a steady-state. The calculation added mass using the Sauerbrey equation might result in an appreciable error.

In Figure 4, we present the sorption results after the dehydrated S8 film was exposed to H_2 gas at varying flow rates. The change in dissipation factor (ΔD) corresponded well with the observed change in ΔF. One would expect that the more H_2 the $Cu_3[Co_2(CN)_6]_2$ film adsorbed, the more energy the film stored during the oscillation.

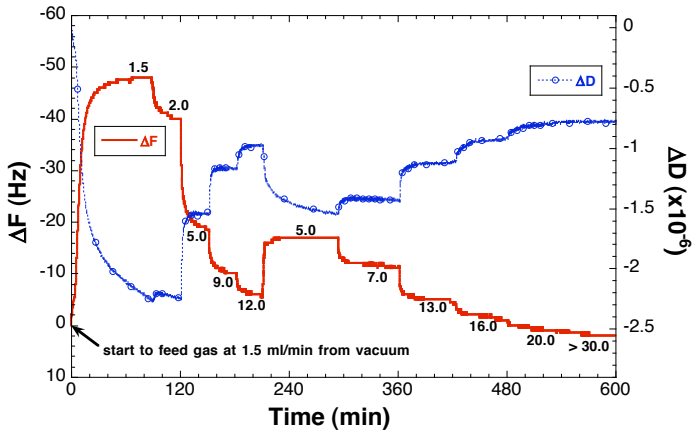

Figure 4. The sorption behavior of S8 when the H_2 flow rate varied between 1.5 and > 30 ml/min (at 23.5 °C and ~ 590 torr) (ΔF3/3 and ΔD3 data).

As the flow rate increased from 2.0 to 5.0 ml/min, the value of ΔF increased from -40 Hz to -17 Hz. When the flow rate decreased from 12.0 ml/min back to 5.0 ml/min, the value of ΔF returned from -5 Hz to -17 Hz. Upon increasing and decreasing the flow rate, there appeared to be some hysteresis effect. However, the same equilibrium point was ultimately reached when the flow conditions are held the same. An increase in flow rate appeared to accelerate the response of the $Cu_3[Co_2(CN)_6]_2$ thin film but appreciably reduced the frequency change (ΔF). When the flow rate was increased above 30 ml/min, the absolute value of ΔF decreases to almost zero. If this were a bulk material, conventional interpretation would suggest that this indicates no appreciable adsorption of H_2 at the ambient pressure, consistent with other researchers' results.[1,3,10]

5. Conclusion

In this work, highly sensitive QCM-D measurements were employed to study H_2 adsorption and desorption in $Cu_3[Co_2(CN)_6]_2$ thin films. The thickness (and presumably morphology) of the $Cu_3[Co_2(CN)_6]_2$ film seems to affect the kinetics of H_2 sorption, but does not influence the equilibrium end-point. However, an apparent H_2 mass uptake as high as 5.0 wt% was detected for the $Cu_3[Co_2(CN)_6]_2$ thin films even at the ambient conditions. While this could be due to an abundance of inter-grain adsorption sites in the polycrystalline thin film, or some other mechanism, this value is surprisingly high and is therefore considered suspect. When the gas flow rate was increased from 0 to > 30 ml/min, the H_2 uptake deduced from changes in frequency appeared to decreases to < 0.02 wt%, which becomes more consistent the literature results. However, it is imaginable that flow-induced forces on the quartz crystal (e.g. drag) could also contribute to the observed flow effect. Therefore, more in-depth study and fundamental understanding about this technique is warranted before it can be used with confidence to conduct gas sorption studies on thin films.

Acknowledgement. This study was funded by the LDRD-DR program of Los Alamos National Laboratory (LANL). We thank the help from Robert Day on the thickness measurement and the help from Ron Martinez on the sorption apparatus modification. We also thank Neil Henson (LANL) and Matthew C. Dixon (Q-sense) for useful discussions and insights about the QCM measurement.

References

1. K. W. Chapman, P. D. Southon, C. L. Weeks and C. J. Kepert, *Chemical Communications*, 3322-3324 (2005).
2. J. Roque, E. Reguera, J. Balmaseda, J. Rodriguez-Hernandez, L. Reguera and L. F. del Castillo, *Microporous and Mesoporous Materials*, **103**, 57-71 (2007).
3. S. S. Kaye and J. R. Long, *Journal of the American Chemical Society*, **127**, 6506-6507 (2005).
4. E. L. Cussler, *Diffusion Mass Transfer in Fluid Systems*, Cambridge University Press, New York, 2002.
5. M. Mulder, *Basic Principles of Membrane Technology*, Kluwer Academic publishers, Dordrecht/Boston/London, 1991.
6. B. D. Vogt, C. L. Soles, H. J. Lee, E. K. Lin and W.-L. Wu, *Langmuir*, **20**, 1453-1458 (2004).
7. F. A. Long, E. Bagley and J. Wilkens, *Journal of Chemical Physics*, **21**, 1412-1413 (1953).
8. I. Ordaz, L. Singh, P. J. Ludovice and C. L. Henderson, *Materials Research Society Symposium Proceedings*, **899**, 52-57 (2005).
9. J. L. C. Rowsell, E. C. Spencer, J. Eckert, J. A. K. Howard and O. M. Yaghi, *Science*, **309**, 1350-1354 (2005).
10. S. Natesakhawat, J. T. Culp, C. Matranga and B. Bockrath, *Journal of Physical Chemistry C*, **111**, 1055-1060 (2007).
11. M. R. Hartman, V. K. Peterson, Y. Liu, S. S. Kaye and J. R. Long, *Chemistry of Materials*, **18**, 3221-3224 (2006).
12 X. Lin, J. H. Jia, P. Hubberstey, M. Schroder and N. R. Champness, *Crystengcomm*, **9**, 438-448 (2007).
13. D. Y. Siberio-Perez, O. M. Yaghi and A. J. Matzger, *AIChE Annual Meeting, Conference Proceedings*, 2336-2336 (2005).
14. J. Hlavay and G. G. Guilbault, *Anal Chem*, **49**, 1890-1898 (1977).
15. R. V. Bucur, V. Mecea and T. B. Flanagan, *Surface Science*, **54**, 477-488 (1976).
16. R. V. Bucur and L. Stoicovi*, *Journal of Electroanalytical Chemistry*, **25**, 342-& (1970).
17. L. M. Webber, J. Hlavay and G. G. Guilbault, *Mikrochimica Acta*, **1**, 351-358 (1978).
18. G. A. Frazier and R. Glosser, *Journal of the Less-Common Metals*, **74**, 89-96 (1980).
19. I. Sasaki, H. Tsuchiya, M. Nishioka, M. Sadakata and T. Okubo, *Sensors and Actuators B (Chemical)*, **B86**, 26-33 (2002).
20. Y. Seo and I. Yu, *Physical Review B*, **60**, 17003 (1999).
21. R. V. Bucur, *Revue Roumaine de Physique*, **24**, 47-56 (1979).
22. R. V. Bucur and V. Mecea, *Surface Technology*, **11**, 305-322 (1980).
23. V. M. Mecea, J. O. Carlsson and R. V. Bucur, *Sensors and Actuators A (Physical)*, **A53**, 371-378 (1996).
24. D. E. Azofeifa, N. Clark, A. Amador and A. Saenz, *Thin Solid Films*, **300**, 295-298 (1997).
25. S. Virji, J. X. Huang, R. B. Kaner and B. H. Weiller, *Nano Letters*, **4**, 491 (2004).
26. A. Z. Sadek, C. O. Baker, D. A. Powell, W. Wlodarski, R. B. Kaner and K. Kalantar-zadeh, *IEEE Sensors Journal*, **7**, 213-218 (2007).
27. G. Bunte, J. Hurttlen, H. Pontius, K. Hartlieb and H. Krause, *Analytica Chimica Acta*, **591**, 49-56 (2007).
28. M. P. Siegal, W. G. Yelton, D. L. Overmyer and P. P. Provencio, *Langmuir*, **20**, 1194-1198 (2004).
29. G. G. Guilbault, J. Affolter, Y. Tomita and E. S. Kolesar, *Analytical Chemistry*, **53**, 2057-2060 (1981).
30. J. F. Alder and J. J. McCallum, *Analyst*, **108**, 1169-1189 (1983).
31. G. G. Guilbault and J. M. Jordan, *CRC Critical Reviews in Analytical Chemistry*, **19**, 1-28 (1988).
32. K. A. Marx, *Biomacromolecules*, **4**, 1099-1120 (2003).
33. G. Sauerbrey, *Zeitschrift fur Physik*, **155**, 206-222 (1959).
34. J. RaviPrakash, A. H. McDaniel, M. Horn, L. Pilione, P. Sunal, R. Messier, R. T. McGrath and F. K. Schweighardt, *Sensors and Actuators B (Chemical)*, **120**, 439-446 (2007).